

We are IntechOpen, the world's leading publisher of Open Access books Built by scientists, for scientists

6,900

Open access books available

186,000

International authors and editors

200M

Downloads

Our authors are among the

154

Countries delivered to

TOP 1%

most cited scientists

12.2%

Contributors from top 500 universities



WEB OF SCIENCE™

Selection of our books indexed in the Book Citation Index
in Web of Science™ Core Collection (BKCI)

Interested in publishing with us?
Contact book.department@intechopen.com

Numbers displayed above are based on latest data collected.
For more information visit www.intechopen.com



Graphical Analysis of Gasification Processes

Shehzaad Kauchali

Abstract

Gasification processes incorporate many reactions that are fairly complex to analyse making their design difficult. In this chapter it is shown that general gasification systems are limited by consideration of mass and energy balances only. Here, a ternary Carbon-Hydrogen-Oxygen diagram is developed to represent gasification processes. The diagram incorporates basic chemistry and thermodynamics to define a region in which gasification occurs. The techniques are further validated from data obtained from pilot or laboratory experiments available in literature. In this chapter we develop graphical representation for sawdust gasification and underground coal gasification (UCG), a clean coal technology. The methods described allow for further analysis without considerations to thermodynamic equilibrium, reactor kinetics, reactor design and operation. This analysis is thus an indispensable tool for flowsheet development using gasification and an excellent tool for practitioners to rapidly understand gasification processes.

Keywords: gasification, biomass, sawdust, CHO-diagram, coal, UCG

1. Introduction

Biomass gasification processes produce a versatile fuel-gas using a thermo-chemical conversion of the biomass in a reducing environment in the presence of air, oxygen or steam. The resulting gas is cleaned and is generally suitable for heating, power generation or liquid fuel production. The important drivers towards biomass utilisation include renewable and sustainable energy sources, the Kyoto protocol addressing the need to lower carbon dioxide emissions and the CO₂-neutrality of biomass emissions. However, it is argued that biomass conversion systems be as efficient as existing fossil fuel technologies [1]. It is stated that gasification is one of the least efficient processes in the biomass-to-energy value chain and a study on the gasifier alone can lead to substantial improvements [2].

Large amounts of literary work, including theoretical and experimental developments, on biomass gasification have been published [3–11].

The use of bond-equivalent percentages to study conversion of coal to other materials on a ternary Carbon-Hydrogen-Oxygen (CHO) diagram has been advocated by [12]. [13] have used a CHO diagram to determine the feasible operating region of a moving bed gasification reactor. In an important follow on work, by [14], it was shown that any coal gasification process can be constrained to a region, by stoichiometry, and further to a line or plane by energy considerations. Thus complex coal gasification reaction schemes can be interpreted readily before the consideration of thermodynamic equilibrium, kinetics, reactor design and

operation. This work forms the basis of the sawdust gasification analysis in this paper. Recently [15] use a graphical targeting approach, on the CHO diagram, to design a biomass gasification process for methanol production. This chapter seeks to provide design options for biomass gasification, on the CHO diagram, in order to evaluate theoretical limitations of the complex reacting systems. Moreover, these options are envisaged to assist in the design of new pilot-scale experiments or commercial operation of biomass and underground coal gasification systems.

There is a lack of coherent approaches to designing gasification processes. This is partly due to the fact that most approaches rely heavily on reactor types, where the information is proprietary and partly due to non-existence of fundamental explanations based on simple chemistry and thermodynamics. It is thus useful to develop a method that enables the understanding of gasification from basic principles. Lastly, and more importantly, it would be useful to empower a designer to suggest experimental validity, for given solid-feedstock, based on preliminary designs derived from the methods discussed in this chapter. This will invariably lead to honing into final designs quicker, with less experimental effort and cost.

The chapter is ordered according to the following: first the bond-equivalent CHO diagram is introduced, followed by the determination of the important gasification reactions and stoichiometric region for sawdust and underground coal gasification, followed by the determination of autothermal operation and the representation of experimental data on the CHO diagram.

2. Bond-equivalent CHO diagram

The bond-equivalent percentages, as introduced by [12], implement the bonding capability of each element in the CHO system. Bond-equivalent percentages spread data points uniformly in the CHO diagram, making analysis visually appealing, and this technique is used for the remainder of the discussions in this work.

2.1 Introduction to CHO diagram

The bond-equivalent CHO diagram is shown in **Figure 1**, below, where the apexes represent pure C, H and O as well as pure C, H₂ and O₂. The other important permanent species that need to be represented are CO₂, CO, H₂, CH₄ and H₂O [5]. For example, to obtain the bond equivalent fraction for a species C_xH_yO_z, the contribution by carbon is 4(x), hydrogen is 1(y) and oxygen is 2(z), which is normalised for each species. Thus CH₄ is represented by C = 4/(4 + 4) and H = 4/(4 + 4) and places the point midway between C and H. Similarly CO₂ and H₂O are midway between C-O and H-O respectively. CO is a third between C-O.

2.2 Representing chemical species and reactions

Chemical species, as individual or in a mixture (such as feed to a process), can thus be represented as single points on the CHO diagram. For example, a synthesis gas of composition 33.3% CO and 67.7% H₂ (CO:2H₂) may be represented as a single COH₄ species and is plotted in **Figure 1**. Dry sawdust represented by CH_{1.35}O_{0.617} [16] is also shown.

A further property of the diagram is that reactions may be represented as intersections of two lines: one representing the reactants and, the other, products. For example, the line joining CH₄ to O₂ intersecting with the line joining CO and H₂ represents partial oxidation of methane to form H₂ and CO, in the ratio 2:1.

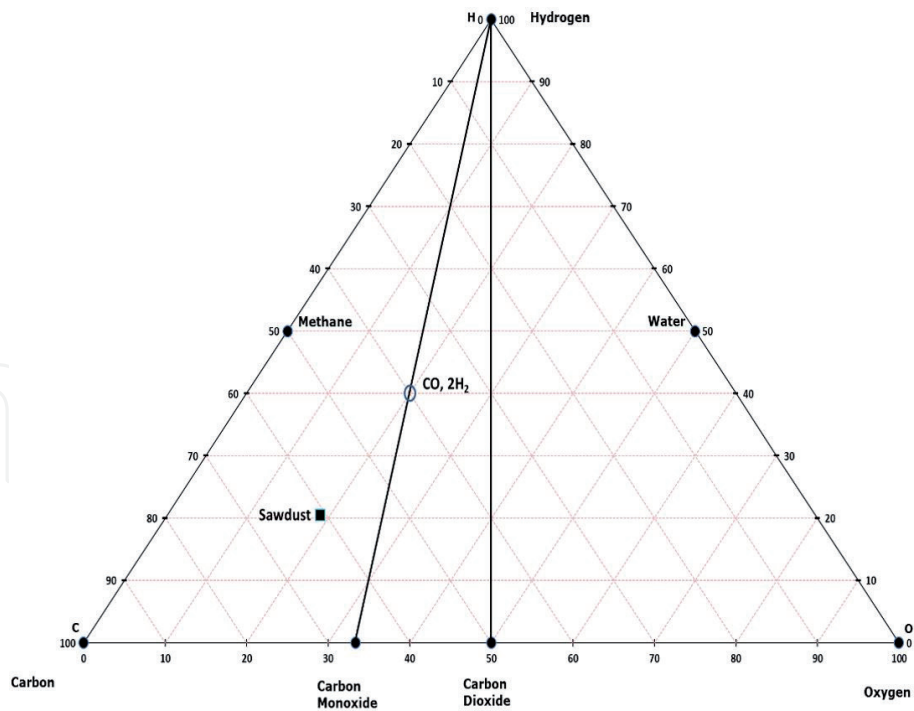


Figure 1.
 Representation of chemical species on the bond equivalent CHO diagram.

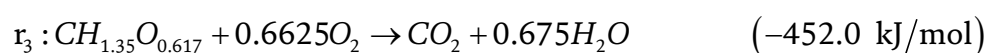
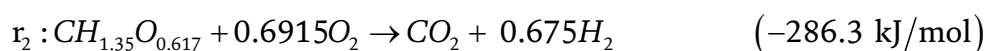
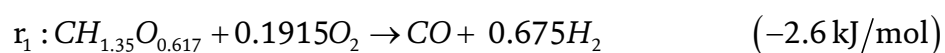
3. Stoichiometric region of operation for sawdust

The analysis performed here utilises dry sawdust with chemical formula $CH_{1.35}O_{0.617}$ with HHV of 476 KJ/mol [16] and a calculated ΔH of formation of -107.77 KJ/mol. The nitrogen, sulphur and other elements (including ash) are considered inerts within the CHO diagram and are excluded from analysis. The theoretical development here seeks to determine the region in the CHO triangle where the gasification of sawdust is feasible and attractive energy-wise. Furthermore, the theoretical result will be compared with those from pilot scale experiments in a later section.

3.1 Stoichiometric region of operation for sawdust

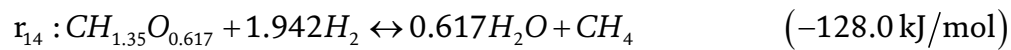
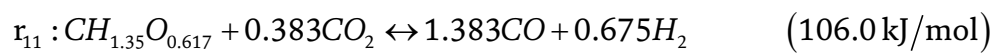
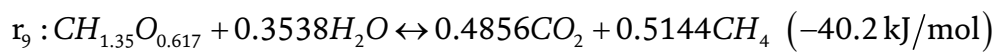
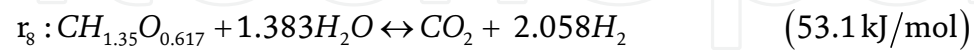
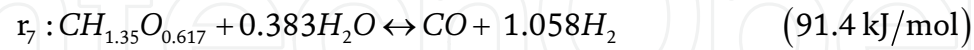
It is acknowledged that gasification reactions are complex comprising of numerous reactions occurring on solid surface or in gas phase. The gasification system considered here comprises of sawdust, steam and oxygen (or air with nitrogen as inert). In contrast, [14] considers a similar system with fixed carbon, steam and oxygen to represent a coal gasification system. Furthermore, a simplified set of reactions are provided that limit the product species from the list of permanent gases (CO , CO_2 , H_2O , CH_4 & H_2) that occur in appreciable amounts between 650 K–1500 K [5].

For the sawdust system, the following reactions at 650 K will thus be considered:
 Combustion





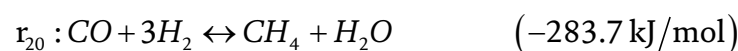
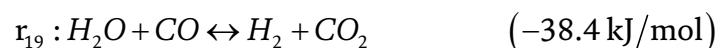
Gasification



Gas combustion



Gas reactions



The reactions (r_1 - r_{16}) are not chosen arbitrarily. The reactions are chosen on the basis that sawdust will react with a number of gases, some from feed (oxygen, steam) while others from primary products such as hydrogen or carbon dioxide.

3.2 Graphical representation of sawdust reactions

The reactions (r_1 - r_{16}) are plotted on the CHO diagram in **Figure 2**. The dotted line represents combustion reactions and the dashed lines are gasification reactions. It is noted that there are no reactions with CH_4 and biomass or CO and biomass as these lines (CH_4 -sawdust & CO-sawdust) do not intersect with any other lines since they are on the extreme edges. There are other reaction schemes plausible that have not been included as they shall not form part of the important subset shown later.

3.2.1 The non-negative basis reactions

From the reactions given above, some reactions are dependent on each other. Furthermore, the gasification system, and hence the analysis, requires only those reactions to form the basis reactions which are able to: 1) obtain other reactions by positive linear combinations, and 2) do not produce the original feed reactants, in particular O_2 , H_2O and C. The reader is directed to [14] for further clarity. The eight important basis reactions that satisfy the two conditions are given in **Table 1**.

A method for determining which reactions are part of the basis set can be described as follows: Firstly, connect all product species, excluding the ones that appear in the feed (steam and oxygen). Note, water-methane, water-carbon dioxide and water-carbon monoxide are thus also omitted. Secondly, connect the feed (sawdust) to the feed oxidants (steam and oxygen). The intersections that are formed (within the diagram – excluding edges) are the basis reactions where the connected points form the reactants and products respectively. Also note hydrogen is not forming part of the reactants in the basis reactions as it is not specified as a feed and thus is excluded.

Any sawdust gasification overall reaction can be obtained by positive linear combinations of the eight basis reactions in **Table 1**. This is translated graphically by implying that an interior point in the space (formed by the basis reactions) can be obtained by connecting any boundary points.

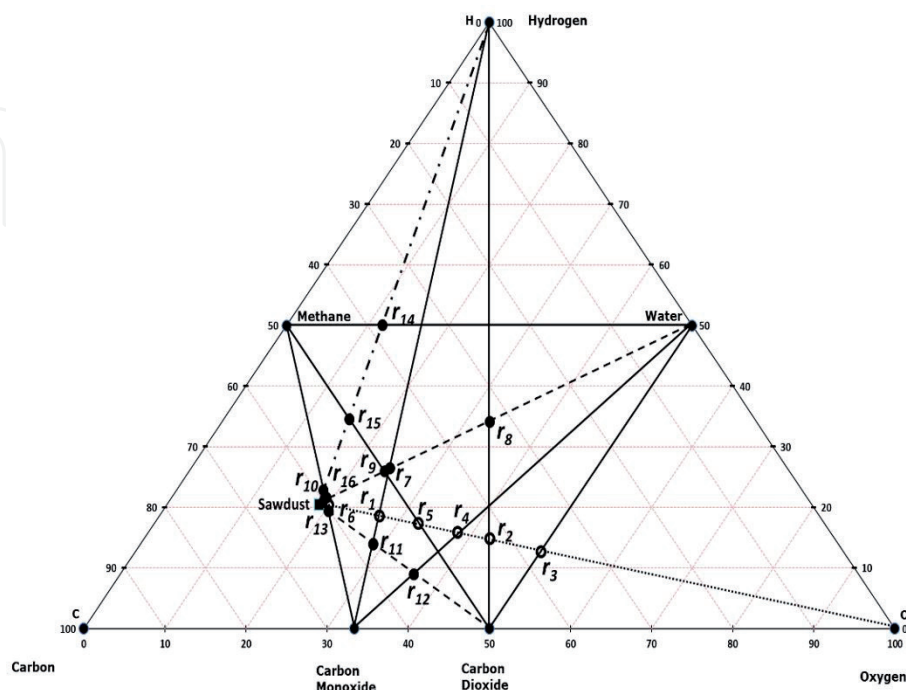


Figure 2.
 Graphical representation of sawdust reactions.

Table 1 summarises the important reactions between sawdust, oxygen and steam. Notice, the reactions also represent the line, which in turn, determine the reactants or products. This is shown in **Figure 3**. For example, a line representing the reactants (sawdust and oxygen) is obtained by connecting the sawdust point with the pure oxygen point. However, the products obtained from this reactant line (sawdust-oxygen) are dependent on which product line is intersected. The product line is one which contains two of the permanent gases listed previously. For illustration purposes, consider the two product lines obtained from H_2 -CO and H_2 -CO₂ – these are strictly products as none of them feature in the feed given. Finally, to obtain the reactions, say r_1 , the intersection of the lines joining sawdust-oxygen and CO- H_2 are considered. In **Figure 3**, this intersection point is presented by point A. It also represents the bond equivalent point plotted for either the feed or product. The relevant stoichiometric values are then used to balance the reaction and are listed in **Table 1**. The process was thus repeated for all possible intersection points and a set of balanced reactions were obtained (r_1 - r_{16}). Moreover, the heat of reactions were determined based on the balanced reactions. The values have been provided in brackets after every reaction. Whilst, the reactions are not meant to represent reaction sequence or mechanism they do provide for a macro representation of the possible outputs from a sawdust gasification system. This is useful when predictions of syngas composition is critical for design.

| | |
|--|-------------------|
| $r_1 : CH_{1.35}O_{0.617} + 0.1915O_2 \rightarrow CO + 0.675H_2$ | (-2.6 kJ / mol) |
| $r_2 : CH_{1.35}O_{0.617} + 0.6915O_2 \rightarrow CO_2 + 0.675H_2$ | (-286.3 kJ / mol) |
| $r_8 : CH_{1.35}O_{0.617} + 1.383H_2O \leftrightarrow CO_2 + 2.058H_2$ | (53.1 kJ / mol) |
| $r_7 : CH_{1.35}O_{0.617} + 0.383H_2O \leftrightarrow CO + 1.058H_2$ | (91.4 kJ / mol) |
| $r_5 : CH_{1.35}O_{0.617} + 0.354O_2 \rightarrow 0.6625CO_2 + 0.3375CH_4$ | (-181.8 kJ / mol) |
| $r_6 : CH_{1.35}O_{0.617} + 0.02275O_2 \rightarrow 0.6625CO + 0.3375CH_4$ | (6.2 kJ / mol) |
| $r_9 : CH_{1.35}O_{0.617} + 0.3538H_2O \leftrightarrow 0.4856CO_2 + 0.5144CH_4$ | (-40.2 kJ / mol) |
| $r_{10} : CH_{1.35}O_{0.617} + 0.0303H_2O \leftrightarrow 0.6473CO + 0.3527CH_4$ | (14.0 kJ / mol) |

Table 1.
Non-negative basis reactions for sawdust.

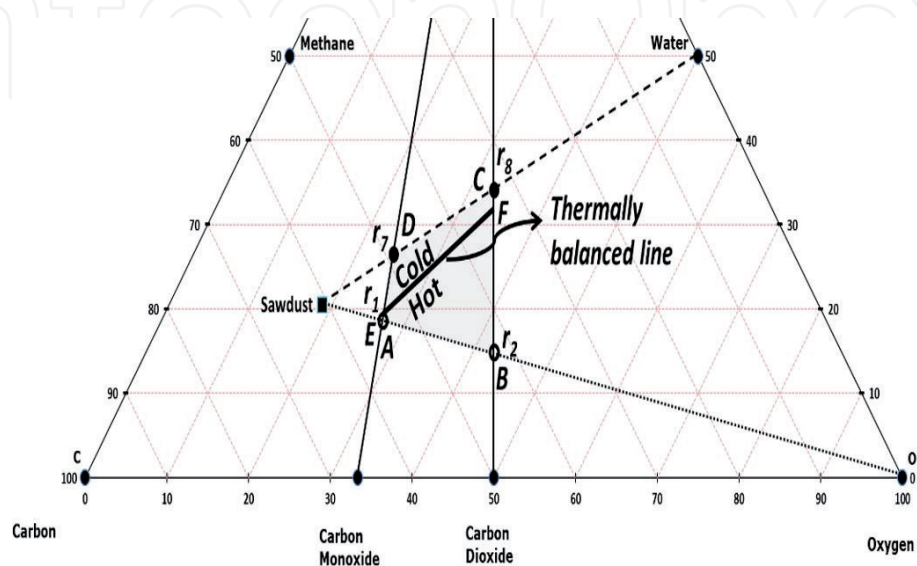


Figure 3.
Stoichiometric region for sawdust without methane formation.

The heat of reactions listed with the various reactions are important as they provide the necessary energy for gasification processes to occur. It is noted that some heat of reactions are endothermic (positive) and some exothermic (negative). Of particular interest are the heat of reactions for r_6 , r_9 and r_{10} . r_9 depicts the exothermic nature of steam reaction producing syngas rich in CO_2 and CH_4 – this has not been reported elsewhere and is of commercial interest requiring low temperature (<400C) and perhaps even the use of catalysts. r_6 and r_9 both demonstrate the lowest amount of oxygen and steam required to gasify sawdust, to produce syngas rich in CO and CH_4 , at high temperatures and non-catalytically.

The sawdust-oxygen intersection with the product lines were depicted in **Figure 2**. These are represented, in order from the sawdust point, by r_6 , r_1 , r_5 , r_4 , r_2 and r_3 . Of these points, it is noted that r_3 and r_4 do NOT form part of the basis reactions as one of the products (water) is already accounted for in the feed. This leaves only reactions that form either one of the products: CO , CO_2 , H_2 and CH_4 . The same analysis applied to sawdust-water intersections with the product lines requires that those reactions that produce only the products CO , CO_2 , H_2 and CH_4 are included.

For most gasification systems, the compositions of the syngas desired is dependent on the end use for the gas. For example for liquid chemicals production syngas rich in H_2 and CO , with minimal CH_4 , is required. The system can be designed for low methane production. When methane is not formed, then only the first four reactions (**Table 1** and region ABCD in **Figure 3**) will provide the possible products obtainable from the gasification system using sawdust, oxygen and steam. This fundamentally implies that any sensible gasification (conversion of sawdust to gas with significant calorific value/energy content) will occur inside the stoichiometric region ABCD. Operating outside of this region will result in material not converted in the gasification process and leave the gasifier unreacted – which is not a preferred mode of operation.

3.2.2 Stoichiometric regions without methane reactions

When methane reactions are excluded from the reactor product, such as required for liquid fuel or chemicals production, the basis reactions as from **Table 1**, form a region (ABCD) as shown in **Figure 3**, above. It is noted that these reactions, which form part of the extreme boundary, span all sensible gasification products within the region. Any interior point inside region ABCD can be obtained by linear combinations of reactions r_1 , r_2 , r_7 and r_8 where the final products will be a combination of H_2 , CO and CO_2 only. Moreover, the edges of the region comprise of oxygen (air) gasification processes, on the lower side (AB), and steam gasification (CD) on the top side of ABCD. Furthermore, these reactions are chosen on the initial premise that no product should contain any reactant, hence any reaction that forms steam (or oxygen) is automatically rejected. Also, operation of a gasification system to the left of AD implies that the feed contains more sawdust than steam and oxygen, which inherently implies that unreacted sawdust should be expected at the exit of the reactor. Similarly, operating to the right of BC implies that the feed contains more steam/oxygen which will leave the gasifier unreacted, implying non-optimal usage of steam/oxygen. It is in this context that it is implied that sensible gasification occurs within the region ABCD. The case where methane is formed is omitted from further interpretation and will form part of a future publication.

4. Autothermal operation

When gasifiers run under adiabatic conditions, without heat loss or added heat, the system balances the exothermic reactions with the endothermic reactions. In

| | |
|---|-------------|
| E: $CH_{1.35}O_{0.617} + 0.186O_2 + 0.0107H_2O \rightarrow CO + 0.686H_2$ | (0kJ / mol) |
| F: $CH_{1.35}O_{0.617} + 0.108O_2 + 1.17H_2O \rightarrow CO_2 + 1.84H_2$ | (0kJ / mol) |

Table 2.
Thermally balanced basis reactions without methane formation.

Figure 3, the two exothermic reactions r_1 and r_2 can be used to balance the endothermic reactions r_7 & r_8 . Line EF forms the thermally balanced line and the product temperature equals the inlet temperature. The thermally balanced equations for reactions E and F are given in **Table 2** for the case where no methane forms.

When methane is not produced, any thermally balanced process can be obtained by the linear combination of the two thermally balanced basis reactions. In **Figure 3**, below line EF products emerge hotter, while above the line they are colder. Furthermore, point E is preferred under low H_2O/O_2 ratios while F would be preferred for high H_2O/O_2 ratios. According to [14] practical gasification processes occur below the thermally balanced line and on the hot side. The reason is a combination of compensation for heat losses as well as methanation in real gasification systems. Operating in the colder section is an indication of external heat sources used to drive the endothermic reactions. Section 6 looks at some experimental points for sawdust gasification in relation to the thermally balanced line EF.

5. Carbon boundary and contours of higher heating value

The work of [17] studied the effect of temperature and pressure on carbon formation in gasification systems. It was identified that it is common for carbon to partially gasify and, due to kinetic limitations, solid carbon does not achieve equilibrium. Furthermore, the carbon boundary, under thermodynamic limits, may be represented on the CHO diagram as isotherms at constant pressure. Two such isotherms have been depicted in **Figure 4** at 1000 K [7] and 733 K [5]. Operating a

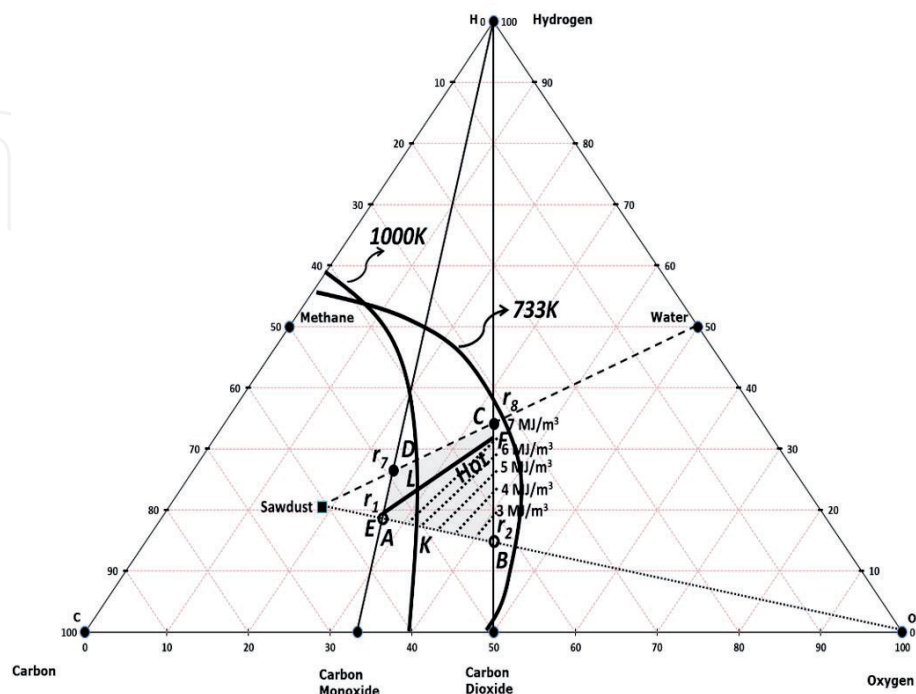


Figure 4.
Carbon boundaries at 733 K and 1000 K with HHV contours.

gasification process within the carbon boundary indicates that there is a propensity for unreacted carbon to occur in the product stream.

This results in low carbon conversions with some carbon remaining in the ash. Moreover, it is desirable to operate in a carbon-free region. In **Figure 4**, it is evident that operating a process with feed within the stoichiometric region ABCD, at low temperatures (733 K), will invariably lead to carbon deposition. It is therefore important to determine the average maximum temperature achievable in the gasification system in order to assess the location of the carbon boundary. **Figure 4** also shows a carbon boundary for a system that operates at 1000 K. The presence of the high temperature carbon boundary further reduces the stoichiometric region in which it is desirable to operate a gasification system. For exothermic gasification, with 100% carbon conversion, it is favourable to operate in the region defined by KBFL (**Figure 4**). **Figure 4** also shows the calorific value (HHV) contours (3–7 MJ/m³) for the idealised stoichiometric region when only air (Nitrogen 79%) is used. These contours are useful when deciding on the targeted calorific value of the product syngas as well as air and steam requirements.

6. Representation of experimental points for sawdust gasification

Tables 3–5 summarise some experimental data available for analysis on the CHO-diagram. It is notable to see that the fuels used have similar C,H and O content. In this analysis the chemical representation of [16] was used to determine

| Reference | Comments | Gasifier type | Sawdust chemical formula (dry, ash-free) | | |
|----------------------|---|---------------------------|--|------|-------|
| | | | C | H | O |
| Basu [16] | Basis for Heat of Reaction calculations | | 1 | 1.35 | 0.617 |
| Li et al. [7] | Syngas data from Figure 15. 4 extreme points taken from set of 15 experimental runs. Average sawdust composition reported from 7 wood species | Circulating Fluidised Bed | 1 | 1.55 | 0.597 |
| Zainal et al. [10] | Calculated from modelled data in Table 5 (Dry gas) including steam in product stream | Fixed Bed Downdraft | 1 | 1.44 | 0.66 |
| Li et al. [18] | Calculated from Figure 2a (S/B = 0.8) including steam in product stream | Circulating Fluidised Bed | 1 | 1.46 | 0.75 |
| Qin et al. [19] | Calculated from Figure 15 (1400C) including steam in product stream | Entrained Flow | 1 | 1.53 | 0.66 |
| Fletcher et al. [20] | CFD modelling of gasifier | Entrained Flow | 1 | 1.68 | 0.6 |
| Meng et al. [21] | Calculated from Figure 2 (S/B = 0.8 & 2.9) including steam in product stream. Representation of 8 experimental points | Bubbling Fluidised Bed | 1 | 1.39 | 0.79 |

Table 3.
 Sawdust characterisation and gasifier type used from literature.

| Reference | Mol composition (syngas) | | | Syngas composition (mol %) | | | | | |
|----------------------|--------------------------|------|------|----------------------------|------|-----------------|-----------------|------------------|-------------------------------|
| | C | H | O | H ₂ | CO | CO ₂ | CH ₄ | H ₂ O | C ₂ H ₄ |
| Basu [16] | | | | — | — | — | — | — | — |
| Li et al. [7] | 18.5 | 39.0 | 42.6 | — | — | — | — | — | — |
| | 24.6 | 29.8 | 45.6 | | | | | | |
| | 21.0 | 39.6 | 39.5 | | | | | | |
| | 24.8 | 36.4 | 38.8 | | | | | | |
| Zainal et al. [10] | | | | 31.9 | 30.5 | 18.2 | 0.2 | 19.2 | — |
| Li et al. [18] | | | | 13.1 | 23.3 | 14.8 | 8.0 | 40.8 | — |
| Qin et al. [19] | | | | 24.3 | 26.6 | 11.1 | — | 38.0 | — |
| Fletcher et al. [20] | | | | 24.0 | 13.0 | 14.0 | 5.0 | 11.0 | — |
| Meng et al. [21] | | | | 13.9 | 23.8 | 7.8 | 4.4 | 47.5 | 2.6 |
| | | | | 9.9 | 9.3 | 5.4 | 1.9 | 72.7 | 0.8 |

Table 4.
Syngas data from various experimental runs.

| Reference | Bond equivalent composition (syngas) | | |
|----------------------|--------------------------------------|------|------|
| | C | H | O |
| Basu [16] | — | — | — |
| Li et al. [7] | 0.38 | 0.22 | 0.40 |
| | 0.48 | 0.22 | 0.29 |
| | 0.41 | 0.19 | 0.39 |
| | 0.47 | 0.18 | 0.35 |
| Zainal et al. [10] | 0.42 | 0.22 | 0.36 |
| Li et al. [18] | 0.36 | 0.27 | 0.37 |
| Qin et al. [19] | 0.39 | 0.24 | 0.37 |
| Fletcher et al. [20] | 0.39 | 0.28 | 0.33 |
| Meng et al. [21] | 0.34 | 0.31 | 0.35 |
| | 0.16 | 0.41 | 0.43 |

Table 5.
Bond equivalent composition for syngas from various experiments.

the heat of reaction for sawdust and used subsequently for all the other reactions in the respective calculations. It is also noted, that the experimental results have been performed in various types of gasifiers ranging from fixed bed, circulating, entrained flow reactors and even catalytic systems.

Sawdust gasification tests in a pilot-scale air blown circulating fluidized bed gasifier have been performed by [7]. 15 runs were performed with over 6 species of sawdust (with varying moisture content) at atmospheric pressure and temperature ranging from 700–815°C. With air as gasification medium, syngas contaminated with nitrogen was produced with dry gas heating values ranging from 2.43–4.82 MJ/m³ (STP) and 3.59–6.13 MJ/m³ (STP) if tar and light hydrocarbons are produced. A CHO diagram was used to analyse the experiments relative to the carbon boundaries with the conclusion that there are kinetic limitations restricting the full conversion of carbon. **Figure 5** depicts the collection of extreme

by a single straight line in **Figure 5**. It is noted that excess steam has been used and hence the points lie out of the stoichiometric region (grey shaded region). The product syngas is then further dehydrated in an additional step to obtain the dry gas reported by [21].

The CHO diagram development and the analysis performed in this work have thus been validated by experimental data. In summary, sensible biomass gasification systems will operate in a well-defined mass balance region (grey shaded region ABCD in **Figure 5**). This region is further divided by the presence of the energy balance and the carbon boundary (derived from maximum temperature achievable for gasification). With the additional information of the HHV contours, a desirable operating point (for high HHV syngas) can be determined at the intersection of the thermally balanced line and the carbon boundary (maximum gasification temperature). The experimental points from literature also confirm the operational regions for sawdust gasification. Hence, preliminary designs or experimental programs can greatly benefit as a targeted approach is used prior to expensive trials.

7. Equilibrium and thermodynamics

While the basis reactions in **Table 1** provide the necessary process schemes required for gasification, they do not explicitly say how the specific stoichiometry is to be obtained. The restricting factor here is thermodynamic equilibrium limitations and, in the case of [7], kinetic limitations. In general, some aspects of gasification processes may be modelled as equilibrium systems. However, thermodynamics restricts the theoretically achievable CO:H₂ ratios as required by the ideal stoichiometric region. For example, if reaction F is desired at say 1000 K, the equilibrium compositions are H₂O: 0.19, CO:0.19, CO₂:0.16, H₂:0.44 and negligible CH₄. In this case we are seeking a ratio (CO:H₂) of infinity instead of the one limited by thermodynamics at 2.3. In order to achieve the composition from the idealised stoichiometric region steam injection (for H₂ deficient gas) or CO₂ (for CO deficient gas) addition is required to adjust the ratios of the species in the Water-Gas-Shift (WGS) reaction.

7.1 Circumventing thermodynamic limitations using WGS reaction

It is possible to use steam injection to obtain the thermally balanced reaction (F) (**Table 2**). This is in accordance with the Water-Gas-Shift reaction: $\text{CO} + \text{H}_2\text{O} \leftrightarrow \text{CO}_2 + \text{H}_2$. Steam is added to increase H₂ content from a CO rich equilibrium steam. Conversely, CO₂ may be added to increase CO content from a H₂ rich stream although it is not commonly practiced. In this particular case, at 1000 K, the steam per mol of sawdust is >55. This means that a large quantity of steam needs to be raised and condensed after the gasifier. Although this ratio (55) is an extreme case, it is commonly found that ratios of up to 3–7 are used in practice. It is also noted here that the steam assists in obtaining the stoichiometry of the basis reactions and is recycled after the gasifier in a recycle loop comprising of steam generation, condensation, treatment and make-up water stream.

8. Application to underground coal gasification (UCG)

UCG, a clean coal technology, is widely understood as a disruptive mining method that is efficient and environmentally benign. This method extracts deep and stranded coal by performing complex gasification reactions in-situ within the

coal seam. The products of UCG are exactly the same as a surface gasifier without the ash component which is designed to be left underground. Whilst the literature on UCG technology is vast, in this chapter the analysis is limited to the syngas products and region of gasification as demonstrated by CHO-diagram. As an example, consider two UCG projects in Australia performed on Macalister Coal Seam at Bloodwood Creek and Chinchilla.

8.1 Analysis of UCG at Bloodwood Creek and Chinchilla

Macalister Coal Seam, $\text{CH}_{0.898}\text{O}_{0.108}$, has a heat of formation of -112.27 kJ/mol . With this information it can be shown (developed elsewhere), that 8 non-negative basis reactions are possible if the coal is gasified with oxygen and steam where methane production is allowed in the product stream. Furthermore, only 4 independent reactions lead to the thermally balanced operation where the heat of reactions are zero. These reactions are represent in **Table 6** and the thermally balanced region (shaded in grey) in **Figure 6**.

8.2 Representation of UCG processes at Bloodwood Creek and Chinchilla

Figure 6 represents the gasification tendencies for the Macalister Coal Seam, oxygen and steam. The shaded region indicates where the thermally balanced region is for the coal, representing a net zero input/output of energy into the gasifier – a preferred scenario for any ideal gasification process. The Chinchilla syngas output are represented by the triangles and the cross represents Bloodwood Creek

| No. | Reaction |
|-----|---|
| G | $\text{CH}_{0.898}\text{O}_{0.108} + 0.4476\text{O}_2 \rightarrow 0.9964\text{CO} + 0.0036 \text{CO}_2 + 0.4489 \text{H}_2$ |
| H | $\text{CH}_{0.898}\text{O}_{0.108} + 1.167 \text{H}_2\text{O} + 0.3623 \text{O}_2 \rightarrow \text{CO}_2 + 1.6159 \text{H}_2$ |
| I | $\text{CH}_{0.898}\text{O}_{0.108} + 0.5251 \text{H}_2\text{O} + 0.1962 \text{O}_2 \rightarrow 0.487 \text{CH}_4 + 0.513 \text{CO}_2$ |
| J | $\text{CH}_{0.898}\text{O}_{0.108} + 0.3494 \text{O}_2 \rightarrow 0.2244 \text{CH}_4 + 0.0317 \text{CO}_2 + 0.7438 \text{CO}$ |

Table 6.
 Thermally balanced reactions for Macalister coal.

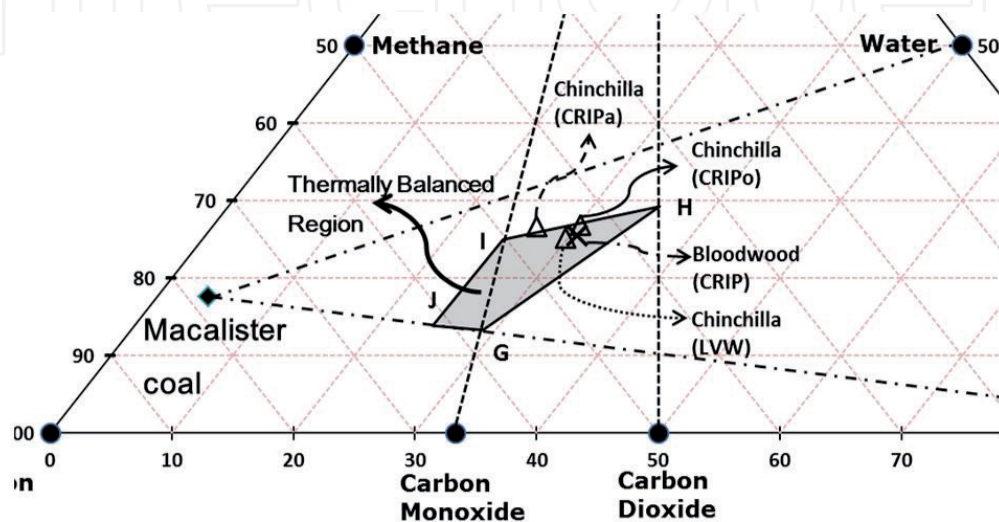


Figure 6.
 Representation of gasification region for Macalister underground coal gasification.

respectively. Two different UCG techniques have been used: Linked Vertical Wells (LVW) and Controlled Retractable Injection Point (CRIP) [22].

The syngas compositions may be found in the works of [22]. It is noted that the output from the UCG field trials lie within the theoretically predicted shaded thermally balanced region. The choice of where to operate the UCG process depends on the final use of the syngas. In these trials, a syngas feed for liquid-fuel production was desired – hence a higher hydrogen to carbon monoxide ratio was required which is achievable around the line HI. For power generation, a syngas with a higher calorific value gas would be required and would thus operate closer to line JI which is richer in methane, carbon monoxide and hydrogen.

9. Conclusions

While gasification systems are complex, the important reactions are represented by basis reactions that span the stoichiometric region of operation on a CHO diagram. The operation of autothermal sawdust gasification systems, without methane formation, is further represented by a line within the stoichiometric region. It is verified, from pilot plant data for gasification of sawdust that the operation occurs within the stoichiometric region and on the hot-side of the thermally balanced line. The analysis in this chapter thus enables the determination of outputs from sawdust gasification which can further be used to design downstream processes. It is shown that a desirable point to operate an air–steam gasification system for power generation (syngas with highest HHV) lies at the point of intersection between the thermally balanced line and the carbon boundary. This intersection represents the point where the maximum HHV is obtained for the gasification system.

The application of the CHO-diagram has been extended to underground coal gasification processes where thermally balanced regions for a given coal was developed. Field trial data were then plotted and found to be in the theoretically predicted thermally balanced region.

The method developed in this chapter provide a high-level analysis to practitioners who are doing basic design in gasification processes – it enables some predictions of syngas possible based on the carbon source and possible oxidants. The output is independent of major parameters such as gasifier type, kinetics or reaction parameters. Lastly, the method provides predictions of syngas compositions possible from a gasification system, enabling design tasks to be completed with reasonable accuracy.

Acknowledgements

Acknowledgments are due to the NRF Grant No. 81248 for funding this work.

IntechOpen

IntechOpen

Author details

Shehzaad Kauchali
School of Chemical and Metallurgical Engineering, University of the
Witwatersrand, Johannesburg, South Africa

*Address all correspondence to: shehzaad.kauchali@wits.ac.za

IntechOpen

© 2021 The Author(s). Licensee IntechOpen. This chapter is distributed under the terms of the Creative Commons Attribution License (<http://creativecommons.org/licenses/by/3.0>), which permits unrestricted use, distribution, and reproduction in any medium, provided the original work is properly cited. 

References

- [1] Prins MJ, Ptasinski KJ, Janssen FJJG. From coal to biomass gasification: Comparison of thermodynamic efficiency. *Energy*. 2007;**32**:1248-1259
- [2] Ptasinski KJ, Prins MJ, Pierik A. Exergetic evaluation of biomass gasification. *Energy*. 2007;**32**:568-574
- [3] Melgar A, Pérez JF, Laget H, Horillo A. Thermochemical equilibrium modelling of a gasifying process. *Energy Conversion and Management*. 2007;**48**:59-67
- [4] Ahmed TY, Ahmad MM, Yusup S, Inayat A, Khan Z. Mathematical and computational approaches for design of biomass gasification for hydrogen production: A review. *Renewable and Sustainable Energy Reviews*. 2012;**16**:2304-2315
- [5] Prins MJ, Ptasinski KJ, Janssen FJJG. Thermodynamics of gas-char reactions: first and second law analysis. *Chemical Engineering Science*. 2003;**58**:1003-1011
- [6] Prins MJ, Ptasinski KJ, Janssen FJJG. Exergetic optimisation of a production process of Fischer-Tropsch fuels from biomass. *Fuel Processing Technology*. 2004;**86**:375-389
- [7] Li XT, Grace JR, Lim CJ, Watkinson AP, Chen HP, Kim JR. Biomass gasification in a circulating fluidizing bed. *Biomass and Bioenergy*. 2004;**26**:171-193
- [8] Radwan AM. An overview on gasification of biomass for production of hydrogen rich gas. *Der Chemica Sinica*. 2012;**3**(2):323-335
- [9] Sadaka SS, Ghaly AE, Sabbah MA. Two phase biomass air-steam gasification model for fluidized bed reactors: Part I-model development. *Biomass and Bioenergy*. 2002;**22**:439-462
- [10] Zainal ZA, Ali R, Lean CH, Seetharamu KN. Prediction of a downdraft gasifier using equilibrium modelling for different biomass materials. *Energy Conversion and Management*. 2001;**42**:1499-1515
- [11] Wander PR, Altafini CR, Barreto RM. Assessment of a small sawdust gasification unit. *Biomass and Bioenergy*. 2004;**27**:467-476
- [12] Battaerd HAJ, Evans DG. An alternative representation of coal composition data. *Fuel*. 1979;**58**(2):105-108
- [13] Yoon H, Wei J, Denn MM. Feasible operating regions for roving bed coal gasification reactors. *Ind. Eng. Chem. Process Des. Dev.* 1979;**18**(2):306-312
- [14] Wei J. A stoichiometric Analysis of Coal Gasification. *Ind. Eng. Chem. Process Des. Dev.* 1979;**18**(3):554-558
- [15] Han Shin Tay D, Kok Sum Ng D, Kheireddine H, El-Halwagi M. Synthesis of an integrated biorefinery via the C-H-O ternary diagram. *Clean Techn Environ Policy*. 2011;**13**:567-579
- [16] Basu P. *Biomass Gasification & Pyrolysis: Practical Design & Theory*. Oxford: Elsevier Inc.; 2010
- [17] Li X, Grace JR, Watkinson AP, Lim CJ, Ergudenler A. Equilibrium modelling of gasification: a free energy minimization approach and its application to a circulating fluidized bed coal gasifier. *Fuel*. 2001;**80**:195-207
- [18] Li Y, Yu M, Fan Y, Li R, Yang T, Chi Y. Effects of metal salt catalysts on fluidized bed gasification characteristics of source-collected combustible solid waste. *BioResources*. 2016;**11**(4):10314-10328
- [19] Qin K, Jensen PA, Lin W, Jensen AD. Biomass Gasification Behavior in an

Entrained Flow Reactor: Gas Product
Distribution and Soot Formation.
Energy & Fuels. 2012;**26**(9):5992-6002

[20] Fletcher DF, Haynes BS, Christo FC,
Joseph SD. A CFD based combustion
model of an entrained flow biomass
gasifier. Applied Maths Modelling.
2000;**24**:165-182

[21] Meng F, Ma Q, Wang H, Liu Y,
Wang D. Effect of Gasifying Agents on
Sawdust Gasification in a Novel Pilot
Scale Bubbling Fluidized Bed System.
Fuel. 2019;**249**:112-118

[22] Perkins G. Underground
coal gasification – Part I: Field
demonstrations and process
performance. Progress in Energy and
Combustion Science. 2018;**67**:158-187

IntechOpen